South East Asian J. of Mathematics and Mathematical Sciences
Vol. 18, No. 3 (2022), pp. 101-122

DOI: 10.56827/SEAJMMS.2022.1803.9 **ISSN (Online): 2582-0850**

ISSN (Print): 0972-7752

AN SVIQR EPIDEMIC MODEL FOR COVID-19

Vijai Shanker Verma, Laxman Bahadur Kunwar, Archana Singh Bhadauria and Vikash Rana

Department of Mathematics & Statistics
Deen Dayal Upadhyaya Gorakhpur University, Gorakhpur, (U.P.), INDIA

E-mail : laxman.kunwar@trmc.tu.edu.np

(**Received:** *Sep. 20, 2022* **Accepted:** *Nov. 05, 2022* **Published:** *Dec. 30, 2022)*

Abstract: We have proposed an SVIQR epidemic model for COVID-19 with vaccination in this research. Some fundamental characteristics such as positivity of the solution, boundedness and invariance of the model are analyzed. Expressions for disease-free equilibrium (DFE) and endemic equilibrium (EE) points with certain criteria for existence are derived. Rigorous analysis of the model reveals that associated DFE is locally asymptotically stable whenever the effective reproduction number is less than one. Also, the EE point is stable whenever certain restrictions are satisfied. Sensitivity analysis is performed to identify key parameters that significantly affect the effective reproduction number. Analytical results are illustrated using parameter values and the results are analyzed using numerical simulation which suggests that the disease will eventually die out, particularly if the control measures are implemented above a specified level for a sustained period of time.

Keywords and Phrases: Covid-19, equilibrium points, stability, effective reproduction number, sensitivity index, numerical simulation.

2020 Mathematics Subject Classification: 34D20, 34D23, 34D08.

1. Introduction

Mathematical modelling plays a vital role for understanding disease dynamics and predicting the future scenario of the disease transmission so government may establish policies to control rapid spread of the disease in absence of an effective

vaccine [12]. After the first introduction of the concept of mathematical modelling of infectious disease, many investigators have studied dynamics of infectious diseases using mathematical models like SIR, SIRS, SEIS, SIQS and SEIRS models [5, 6, 15, 20, 22], characterizing the spread patterns of infectious diseases in the real world. Since vaccination is one of the important measures to stop epidemic from spreading, it is also essential to include vaccination effect to infectious disease models [23]. Through vaccination, a person may gain a permanent or temporary immunity.

Due to the occurrence and reoccurrence of a recent communicable infectious disease COVID-19 caused by severe acute respiratory syndrome coronavirus 2 (SARS-CoV-2), the situation of human beings was full of threat and terror. The disease COVID-19 was first detected in December 2019 in Wuhan, China [18]. Numerous mathematical models are being developed to analyze how COVID-19 is spreading throughout the world and forecast how the outbreak will develop [10]. Kunwar [13] utilized fundamental SIR deterministic compartmental model to study the transmission dynamics of COVID-19 in the context of Nepal. Further, Kunwar and Verma [14] studied the dynamics of the coronavirus disease in the context of Nepal using exponential and logistic mathematical models. Bhadauria et al. [3] have used an SIQV mathematical model on COVID-19 considering the effect of contact tracing as well as the virus population in the environment.

Motivated by published literatures on COVID-19, we have proposed a deterministic model introducing vaccinated and quarantined classes in the classical SEIR model. We predict both short- and long-term COVID-19 trends for India in different scenario and it is recommended that country should continue to monitor its control measures to minimize the contact between infected and susceptible populations. The main objective of the work is to explore the influence of control measures and vaccination for the control and elimination of COVID-19 in the ongoing third wave of the coronavirus disease pandemic situation. However, we have carried out the numerical simulation using the parameter values of the coronavirus disease in this study, the model can be applied to study the dynamics of other communicable infectious diseases in developing countries like Nepal, Bhutan, Bangladesh, etc.

2. Model Formulation

In this study, the total population $N(t)$ under consideration at any time t, is grouped into five compartments; susceptible compartment denoted by $S(t)$, in which the people are at risk of infection with disease; vaccinated compartment denoted by $V(t)$, in which the people have got complete dose vaccine; infected compartment denoted by $I(t)$, in which the people may transmit disease, and they may have mild or strong symptoms; quarantined compartment denoted by $Q(t)$, in

which the people have severe symptoms and quarantined or hospitalized for treatment and they have very low transmission capacity and recovered compartment denoted by $R(t)$ containing the people who have recovered from the disease and are free from infection. Thus, we can write $N(t) = S(t)+V(t)+I(t)+Q(t)+R(t)$. The schematic diagram of the SVIQR model for COVID-19 is shown in figure 1.

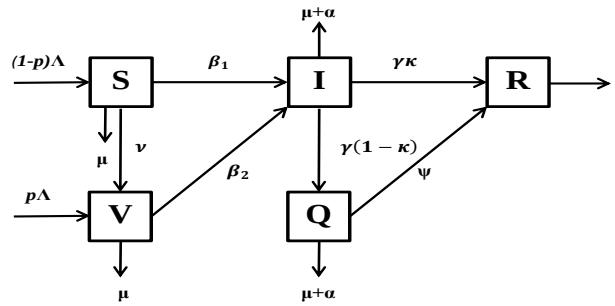

Figure 1: Schematic diagram of the SVIQR model for COVID-19.

The people are recruited into the system with a fixed total recruitment rate Λ among which partly entered into vaccinated and rest into the susceptible compartment. The people of all classes die by natural death rate where as infected and quarantined states have extra mortality rate due to disease. Susceptible and vaccinated people acquire disease infection at rates β_1 and β_2 respectively, where β_1 and β_2 signifies the infection transmission rate of susceptible and vaccinated classes respectively. Also, we assume that $\beta_2 = (1-\epsilon)\beta_1$, where ϵ is the infection reduction of vaccinated individuals. A portion of infected enters into the quarantine class (which includes hospitalized or isolated class) others recover naturally. We assume that recovered individuals gain immunity such that they could not get infected further in the study period. The following system of nonlinear ordinary differential equations makes up the epidemic model that describes the dynamics of COVID-19 which is based on the model flow diagram shown in Figure 1.

$$\left.\begin{aligned}
\frac{dS(t)}{dt} &= (1-p)\Lambda - \beta_1 IS - (\mu+\nu)S,\\
\frac{dV(t)}{dt} &= p\Lambda + \nu S - \beta_2 IV - \mu V,\\
\frac{dI(t)}{dt} &= \beta_1 IS + \beta_2 IV - (\mu+\alpha+\gamma)I,\\
\frac{dQ(t)}{dt} &= (1-\kappa)\gamma I - (\mu+\alpha+\psi)Q,\\
\frac{dR(t)}{dt} &= \gamma\kappa I + \psi Q - \mu R
\end{aligned}\right\} \tag{1}$$

We employ the following notations for convenience : $d_1 = \mu + \nu, d_2 = \mu, d_3 = \mu + \alpha + \gamma$ and $d_4 = \mu + \alpha + \psi$. Therefore, our model is reduced to the following form:

$$\left.\begin{aligned} \frac{dS(t)}{dt} &= (1-p)\Lambda - \beta_1 IS - d_1 S, \\ \frac{dV(t)}{dt} &= p\Lambda + \nu S - \beta_2 IV - d_2 V, \\ \frac{dI(t)}{dt} &= \beta_1 IS + \beta_2 IV - d_3 I, \\ \frac{dQ(t)}{dt} &= (1-\kappa)\gamma I - d_4 Q, \\ \frac{dR(t)}{dt} &= \gamma\kappa I + \psi Q - d_2 R \end{aligned}\right\} \tag{2}$$

with the initial conditions:

$$S(0) = S_0 > 0, V(0) = V_0 \geq 0, I(0) = I_0 \geq 0, Q(0) = Q_0 \geq 0, R(0) = R_0 \geq 0 \tag{3}$$

Table 1: The description of parameters and their values used for simulation.

Parameter	**Description**	**Source**
$\Lambda = 30$	The total recruitment rate	[1]
$p = 0.05$	Proportion of recruitted individuals who are vaccinated	Assumed
$\beta_1 = 0.002$	Infection transmission rate among susceptible individuals	[1]
$\beta_2 = 0.0004$	Infection transmission rate among vaccinated individuals	[1]
$\mu = 0.009$	Natural death rate	[21]
$\alpha = 0.25$	Disease-induced death rate	[21]
$\psi = 0.0701$	Recovery rate of quarantined individuals	[11]
$\nu = 0.3$	Vaccination rate	Assumed
$\gamma = 0.0833$	Recovery rate of infectious class	[2]
$\kappa = 0.05$	Proportion of infectious who recover naturally	[7]
$\epsilon = 0.8$	Vaccine efficacy	Assumed

3. Model Analysis

3.1. Positivity of Solution

Theorem 3.1. *If* $\Omega(t) = \{S(t), V(t), I(t), Q(t), R(t)\}$ *and* $\mathbb{R}^5_+ = \{\Omega(t) \in \mathbb{R}^5 : \Omega(t) \geq 0\}$ *then the solution set* $\Omega(t)$ *of the proposed model (1) together with initial*

condition is non-negative for all $t > 0$ *in* $\mathbb{R}^5_+$.

Proof. From first equation of the system of equations (2), we observe that

$$\frac{dS(t)}{dt} \geq -(\beta_1 I + d_1) S \tag{4}$$

which on integration gives $S(t) \geq S(0) exp\{(-\beta_1 I - d_1) t\}$ which implies that $S(t) \geq 0$ for all $t > 0$.

From second equation of the system of equations (2), we can write

$$\frac{dV(t)}{dt} + [\beta_2 I + d_2] V(t) = p\Lambda + \nu S(t)$$

Solving the above differential equation, we get

$$V(t) exp\left\{d_2 t + \beta_2 \int_0^t I(\tau)\, d\tau\right\}$$
$$= \int_0^t \left[\{p\Lambda + \nu S(y)\} exp\left\{d_2 t + \beta_2 \int_0^y I(\tau)\, d\tau\right\}\right] dy + V(0)$$

$$\therefore \qquad V(t) = \left[V(0) + \int_0^t \left[\{p\Lambda + \nu S(y)\} exp\left\{d_2 t + \beta_2 \int_0^y I(\tau)\, d\tau\right\}\right] dy\right]$$
$$exp\left\{-d_2 t - \beta_2 \int_0^t I(\tau)\, d\tau\right\}$$

which implies that $V(t) \geq 0$.

Proceeding in the similar ways and using same condition, it can be proved that $I(t) \geq 0, Q(t) \geq 0, R(t) \geq 0$, for all $t > 0$.

Hence, the model described by the system of equations (1) is epidemiologically realistic.

3.2. Invariant Region

Here, we establish that the closed region Ω is positively invariant and the proposed model is well posed biologically as well as mathematically within the invariant region Ω.

Theorem 3.2. *The set* Ω *of feasible solutions of the model given by (1) with the initial conditions stated in the region* $\mathbb{R}^5_+$ *is given by*

$$\Omega = \left\{(S(t), V(t), I(t), Q(t), R(t)) \in \mathbb{R}^5_+ : 0 < N(t) \leq \frac{\Lambda}{\mu}\right\}$$

which is positively invariant with respect to the system.

Proof. The total population $N(t)$ at any time t is given as follows:

$$N(t) = S(t) + V(t) + I(t) + Q(t) + R(t) \tag{5}$$

Differentiating (5) and using (2), we get $\frac{dN}{dt} \leq \Lambda - \mu N$
which on integration gives the following expression:

$$N(t) \leq \frac{\Lambda}{\mu} - \left(\frac{\Lambda}{\mu} - N_0\right) exp(-\mu t).$$

where $N_0 = N(0)$ represents the initial population.
Applying the Birkhoff-Rota theorem [4], we find that if $N_0 < \frac{\Lambda}{\mu}$, then $N(t)$ asymptotically tends to $\frac{\Lambda}{\mu}$ as $t \to \infty$.

Hence, all the feasible solutions of system (1) or (2) converge in the region Ω. Therefore, the feasible region for the proposed system is given by

$$\Omega = \left\{(S(t), V(t), I(t), Q(t), R(t)) \in \mathbb{R}_+^5 : 0 < N(t) \leq \frac{\Lambda}{\mu}\right\}$$

3.3. Existence of Disease-Free Equilibrium (DFE)

Since first four equations of the system (1) do not contain variable $R(t)$ i.e. they are free from $R(t)$, therefore we can solve the first four equations of the system (1) and then put the solution values of I and Q in the fifth equation of the system (1). So, we can solve the obtained linear differential equation for variable R independently. Consequently, for $t \to \infty$ we may write the fifth equation as

$$R(t) = \frac{\gamma\kappa I' + \psi Q'}{d_2} \tag{6}$$

where $\left(I', Q'\right)$ refers the solution values of system (1) taking only first four equations.

Now, we study the following reduced system of four equations instead of all five equations of system (1):

$$\left.\begin{aligned} \frac{dS(t)}{dt} &= (1-p)\Lambda - \beta_1 IS - d_1 S, \\ \frac{dV(t)}{dt} &= p\Lambda + \nu S - \beta_2 IV - d_2 V, \\ \frac{dI(t)}{dt} &= \beta_1 IS + \beta_2 IV - d_3 I, \\ \frac{dQ(t)}{dt} &= (1-\kappa)\gamma I - d_4 Q \end{aligned}\right\} \tag{7}$$

Since at the DFE point, infection vanishes from the system, therefore, the DFE point is obtained by solving following system of equations:

$$(1-p)\,\Lambda - \beta_1 IS - d_1 S = 0 \tag{8}$$
$$p\Lambda + \nu S - \beta_2 IV - d_2 V = 0 \tag{9}$$
$$\beta_1 IS + \beta_2 IV - d_3 I = 0 \tag{10}$$
$$(1-\kappa)\,\gamma I - d_4 Q = 0 \tag{11}$$

At the DFE point, there is no infection, so we have $I = 0$. Solving equations (8), (9), (11) and (6), we get the DFE point as $E_1\left(S^0, V^0, I^0, Q^0, R^0\right)$, where

$$S^0 = \frac{(1-p)\,\Lambda}{d_1}, V^0 = \frac{\Lambda\left(pd_2+\nu\right)}{d_1 d_2}, I^0 = 0, Q^0 = 0, R^0 = 0 \tag{12}$$

3.4. Basic Reproduction Number

The basic reproduction number (R_0) is determined at the disease-free equilibrium point. We shall apply the next-generation (spectral radius) matrix method to derive expression for (R_0) [8, 9]. We decompose the right-hand side of the system of equations (1) corresponding to the infected compartments I and Q as $\mathcal{F} - \mathcal{W}$, where

$\mathcal{F} = \begin{bmatrix} \beta_1 IS + \beta_2 IV \\ 0 \end{bmatrix}$ and $\mathcal{W} = \begin{bmatrix} d_3 I \\ -(1-\kappa)\,\gamma I + d_4 Q \end{bmatrix}$,

For the new infectious terms and the remaining transfer terms, the non-negative matrix F and the non-singular matrix W are provided by

$F = \left.\frac{\partial \mathcal{F}}{\partial x_j}\right|_{(E_1)} = \begin{bmatrix} \beta_1 S^0 + \beta_2 V^0 & 0 \\ 0 & 0 \end{bmatrix}$ and $W = \left.\frac{\partial \mathcal{W}}{\partial x_j}\right|_{(E_1)} = \begin{bmatrix} d_3 & 0 \\ -(1-\kappa) & 0 \end{bmatrix}$, for $x_j = I, Q$.

$$\therefore \qquad FW^{-1} = \begin{bmatrix} \frac{1}{d_3}\left(\beta_1 S^0 + \beta_2 V^0\right) & 0 \\ 0 & 0 \end{bmatrix} \tag{13}$$

According to the next generation matrix approach, basic reproduction number is the spectral radius of the matrix FW^{-1}. Here, we have considered the model with implementation of the vaccination as the control strategy. The effective reproduction number $R_0(\nu)$ is defined as the average number of secondary infectious generated by one infectious in a susceptible population when vaccination is implemented. Thus, we get $R_0(\nu)$ for the proposed model (1) as follows:

$$R_0(\nu) = \frac{1}{d_3}\left(\beta_1 S^0 + \beta_2 V^0\right) = \frac{\Lambda\left\{\beta_1 d_2 (1-p) + \beta_2\left(pd_2+\nu\right)\right\}}{d_1 d_2 d_3}$$

$$\therefore \quad R_0(\nu) = \frac{\Lambda\left\{\beta_1 \mu (1-p) + \beta_2\left(p\mu+\nu\right)\right\}}{\mu\left(\mu+\nu\right)\left(\mu+\alpha+\gamma\right)} \tag{14}$$

Also, the effective reproduction number is the basic reproduction number (R_0) with the implementation of intervention so that total population is not susceptible and, therefore, by taking $\nu = 0$, we have

$$R_0 = \frac{\Lambda\left\{\beta_1\left(1-p\right)+\beta_2 p\right\}}{\mu\left(\mu+\alpha+\gamma\right)} \tag{15}$$

3.5. Existence of Endemic Equilibrium (EE)

Theorem 3.3. *If the condition $R_0(\nu) > 1$ holds, then the model described by system (1) has a unique endemic equilibrium.*

Proof. Let $E^*\left(S^*, V^*, I^*, Q^*, R^*\right)$ be endemic equilibrium point, where infectious is always present in the system, i.e. $I^* \neq 0$ and $\frac{dS}{dt} = 0$; $\frac{dV}{dt} = 0$; $\frac{dI}{dt} = 0$; $\frac{dQ}{dt} = 0$.
By $\frac{dS}{dt}\big|_{E^*} = 0$, we have

$$S^* = \frac{\left(1-p\right)\Lambda}{\left(\beta_1 I^* + d_1\right)} \tag{16}$$

By $\frac{dV}{dt}\big|_{E^*} = 0$, we have

$$V^* = \frac{\Lambda\left\{p\left(\beta_1 I^* + d_2\right)+\nu\right\}}{\left(\beta_1 I^* + d_1\right)\left(\beta_2 I^* + d_2\right)} \tag{17}$$

By $\frac{dI}{dt}\big|_{E^*} = 0$, we have

$$I^*\left(\beta_1 S^* + \beta_2 V^* - d_3\right) = 0$$

Since at the EE, $I^* \neq 0$, therefore we must have

$$\beta_1 S^* + \beta_2 V^* - d_3 = 0 \tag{18}$$

By $\frac{dQ}{dt}\big|_{E^*} = 0$, we have

$$Q^* = \frac{\left(1-\kappa\right)\gamma}{d_4} I^* \tag{19}$$

Again, it is noteworthy that R^* is calculated by using equation (6). Hence, the EE point is obtained as $E^*(S^*, V^*, I^*, Q^*, R^*)$, where

$$S^* = \frac{\left(1-p\right)\Lambda}{\left(\beta_1 I^* + d_1\right)}, V^* = \frac{\Lambda\left\{p\left(\beta_1 I^* + d_2\right)+\nu\right\}}{\left(\beta_1 I^* + d_1\right)\left(\beta_2 I^* + d_2\right)}, Q^* = \frac{\left(1-\kappa\right)\gamma}{d_4} I^*, R^* = \frac{\gamma\kappa I^* + \psi Q^*}{d_2}$$

For the existence of unique EE point, we consider equation (18).

Thus, putting the values of S^* and V^* in equation (18), we have

$$-\left(\beta_1\beta_2 d_3\right) I^{*2} + \left(\beta_1\beta_2\Lambda - \beta_1 d_2 d_3 - \beta_2 d_1 d_3\right) I^* + \Lambda\left(q d_2\beta_1 + p d_2\beta_2 + \nu\beta_2\right) - d_1 d_2 d_3 = 0$$

$$i.e. \quad C_1 I^{*2} + C_2 I^* + C_3 = 0 \tag{20}$$

where
$C_1 = -\beta_1\beta_2 d_3 < 0, C_2 = \beta_1\beta_2\Lambda - \beta_1 d_2 d_3 - \beta_2 d_1 d_3$, and $C_3 = \{R_0(\nu) - 1\} d_1 d_2\ d_3$

The quadratic equation (20) in terms of I^* has a unique positive root if and only if the inequality $\frac{C_3}{C_1} < 0$ holds. Since $C_1 < 0$, the required condition takes the form $C_3 > 0$. i.e. $\{R_0(\nu) - 1\} d_1 d_2 d_3 > 0$ or $\{R_0(\nu) - 1\} > 0$ or $R_0(\nu) > 1$.

Hence, there exists a unique positive EE point E^* of the system of equations (7), whenever the condition $R_0(\nu) > 1$ holds.

3.6. Stability Analysis of Disease Free Equilibrium Point

In this section, we shall test the local stability of DFE the system of equations (7) using the linearization technique.

Theorem 3.4. *The disease-free equilibrium point E_1 of the epidemic model given by (1) is locally asymptotically stable if $R_0 < 1$, otherwise unstable.*

Proof. The Jacobian matrix J at DFE point E_1, is given by

$$J(E_1) = \begin{bmatrix} d_1 & 0 & -\beta_1 S^o & 0 \\ \nu & d_2 & -\beta_2 V^o & 0 \\ 0 & 0 & \beta_1 S^o + \beta_2 V^o - d_3 & 0 \\ 0 & 0 & (1-\kappa)\gamma & -d_4 \end{bmatrix}$$

The four eigenvalues of the above Jacobian matrix are found as follows:
$\lambda_1 = -d_2, \lambda_2 = -d_1, \lambda_3 = -d_4$ and $\lambda_4 = \beta_1 S^o + \beta_2 V^o - d_3 = \{R_0(\nu) - 1\} d_3$
Now, since $d_3 > 0$, therefore λ_4 will have negative sign if $R_0(\nu) - 1 < 0$ i.e. $R_0(\nu) < 1$. Thus, all four roots of the characteristic equation of the system (7) at DFE point will have negative real part if $R_0(\nu) < 1$. Therefore, the DFE point is locally asymptotically stable when $R_0(\nu) < 1$, otherwise it will be unstable.

3.7. Stability Analysis of Endemic Equilibrium Point

Theorem 3.5. *The endemic equilibrium point E^* of the system of equations (7), which exists uniquely if $R_0(\nu) > 1$, is locally asymptotically stable under certain restrictions and is unstable otherwise. The restrictions are $A_1 A_2 - A_3 > 0$ and $A_3 > 0$, where A_1, A_2, A_3 are described in the proof.*

Proof. The Jacobian matrix of the system (7) at the EE point E^* is given by

$$J(E^*) = \begin{bmatrix} -(\beta_1 I^* + d_1) & 0 & -\beta_1 S^* & 0 \\ \nu & -(\beta_2 I^* + d_2) & -\beta_2 V^* & 0 \\ \beta_1 I^* & \beta_2 I^* & \beta_1 S^* + \beta_2 V^* - d_3 & 0 \\ 0 & 0 & (1-\kappa)\gamma & -d_4 \end{bmatrix}$$

The first eigenvalue of the above matrix is given by $\lambda_1 = -d_4$ and the remaining eigenvalues are given by the following cubic equation:

$$\lambda^3 + A_1\lambda^2 + A_2\lambda + A_3 = 0 \tag{21}$$

where
$A_1 = x_{11} + x_{22} + x_{33} > 0, A_2 = x_{11}x_{22} + x_{23}x_{32} + x_{13}x_{31} - x_{11}x_{33} - x_{22}x_{33}$,
$A_3 = x_{11}x_{23}x_{32} + x_{13}x_{21}x_{32} + x_{13}x_{31}x_{22} - x_{11}x_{22}x_{33}$; $x_{11} = (\beta_1 I^* + d_1) > 0$;
$x_{13} = \beta_1 S^* > 0; x_{21} = \nu > 0; x_{22} = \beta_2 I^* + d_2 > 0; x_{23} = \beta_2 V^* > 0; x_{31} = \beta_1 I^* > 0$;
$x_{32} = \beta_2 I^* > 0; x_{33} = \beta_1 S^* + \beta_2 V^* - d_3 > 0; x_{43} = (1-\kappa)\gamma > 0$.

By Routh-Hurwitz criterion of order three [19], we can state that all three roots of the equation (21) will consist of negative real parts if conditions $A_1 > 0, (A_1A_2 - A_3)/A_1 > 0$, and $A_3 > 0$ hold. Since $A_1 > 0$, the required conditions are: $A_1A_2 - A_3 > 0$ and $A_3 > 0$.

Hence, all four roots of the characteristic equation of the system (7) at the EE point will have negative real part if $(A_1A_2 - A_3) > 0$ and $A_3 > 0$. Thus, the EE point E^* is locally asymptotically stable when $A_1A_2 - A_3 > 0$ and $A_3 > 0$, otherwise unstable.

Theorem 3.6. *If the endemic equilibrium point $E^*(S^*, V^*, I^*, Q^*, R^*)$ is locally asymptotically stable, then it is globally asymptotically stable, provided that the following conditions hold:*

$$l_{12}^2 < l_{11}l_{22}, l_{13}^2 < \frac{1}{2}l_{11}l_{33}, l_{23}^2 < \frac{1}{2}l_{22}l_{33}, l_{34}^2 < \frac{1}{2}l_{33}l_{44}, l_{35}^2 < \frac{1}{2}l_{33}l_{55}, l_{45}^2 < l_{44}l_{55} \tag{22}$$

where $l_{ij}, (i, j = 1 \ldots 5)$ are described in the proof.

Proof. To derive the condition of globally asymptotically stable of E^*, we consider a Lyapunov function [16], denoted by L and defined as follows :

$$L = \frac{1}{2}(S - S^*)^2 + \frac{1}{2}(V - V^*)^2 + \frac{1}{2}(I - I^*)^2 + \frac{1}{2}(Q - Q^*)^2 + \frac{1}{2}(R - R^*)^2$$

Clearly, $L : \mathbb{R}_+^5 \to \mathbb{R}$. $L(E^*) = 0$ and $L(x) > 0$ whenever $x \neq E^*$. That is, L is a positive definite function.

Now, for the stability of the system at E^*, we have to show that $dL/dt < 0$.

Differentiating L w. r. t. t and applying the condition of EE, we get

$$\begin{aligned}\frac{dL}{dt} = &-\frac{1}{2}\Pi_{11}\left(S-S^*\right)^2 + \Pi_{13}\left(S-S^*\right)\left(I-I^*\right) - \frac{1}{4}\Pi_{33}\left(I-I^*\right)^2 \\ &- \frac{1}{2}\Pi_{11}\left(S-S^*\right)^2 + \Pi_{12}\left(S-S^*\right)\left(V-V^*\right) - \frac{1}{2}\Pi_{22}\left(V-V^*\right)^2 \\ &- \frac{1}{2}\Pi_{22}\left(V-V^*\right)^2 + \Pi_{23}\left(V-V^*\right)\left(I-I^*\right) - \frac{1}{4}\Pi_{33}\left(I-I^*\right)^2 \\ &- \frac{1}{4}\Pi_{33}\left(I-I^*\right)^2 + \Pi_{34}\left(I-I^*\right)\left(Q-Q^*\right) - \frac{1}{2}\Pi_{44}\left(Q-Q^*\right)^2 \\ &- \frac{1}{4}\Pi_{33}\left(I-I^*\right)^2 + \Pi_{35}\left(I-I^*\right)\left(R-R^*\right) - \frac{1}{2}\Pi_{55}\left(R-R^*\right)^2 \\ &- \frac{1}{2}\Pi_{33}\left(Q-Q^*\right)^2 + \Pi_{45}\left(Q-Q^*\right)\left(R-R^*\right) - \frac{1}{2}\Pi_{55}\left(R-R^*\right)^2\end{aligned}$$

where
$\Pi_{11} = \beta_1 I + d_1, \Pi_{22} = d_2 + \beta_2 I^*, \Pi_{33} = d_3 - \beta_1 S - \beta_2 V, \Pi_{44} = d_4, \Pi_{55} = d_2, \Pi_{12} = \nu, \Pi_{13} = \beta_1 I^* - \beta_1 S^*, \Pi_{23} = \beta_2 I^* - \beta_2 V, \Pi_{34} = (1-\kappa)\gamma, \Pi_{35} = \gamma\kappa, \Pi_{45} = \psi$

Now, using condition (22), we obtain the following:

$$\begin{aligned}\frac{dL}{dt} = &-\left[\left\{\sqrt{\frac{\Pi_{11}}{2}}\left(S-S^*\right)\right\} - \left\{\sqrt{\frac{\Pi_{22}}{2}}\left(V-V^*\right)\right\}\right]^2 \\ &-\left[\left\{\sqrt{\frac{\Pi_{11}}{2}}\left(S-S^*\right)\right\} - \left\{\sqrt{\frac{\Pi_{33}}{4}}\left(I-I^*\right)\right\}\right]^2 \\ &-\left[\left\{\sqrt{\frac{\Pi_{22}}{2}}\left(V-V^*\right)\right\} - \left\{\sqrt{\frac{\Pi_{33}}{4}}\left(I-I^*\right)\right\}\right]^2 \\ &-\left[\left\{\sqrt{\frac{\Pi_{33}}{4}}\left(I-I^*\right)\right\} - \left\{\sqrt{\frac{\Pi_{44}}{2}}\left(Q-Q^*\right)\right\}\right]^2 \\ &-\left[\left\{\sqrt{\frac{\Pi_{33}}{4}}\left(I-I^*\right)\right\} - \left\{\sqrt{\frac{\Pi_{55}}{2}}\left(R-R^*\right)\right\}\right]^2 \\ &-\left[\left\{\sqrt{\frac{\Pi_{44}}{2}}\left(Q-Q^*\right)\right\} - \left\{\sqrt{\frac{\Pi_{55}}{2}}\left(R-R^*\right)\right\}\right]^2 < 0\end{aligned}$$

where
$l_{12} = \nu, l_{11} = d_1, l_{22} = d_2 + \beta_2 I^*, l_{13} = \beta_1 I^* - \beta_1 S^*, l_{33} = d_3 - (\beta_1 + \beta_2)\frac{\Lambda}{\mu}$,
$l_{23} = \beta_1 I^*, l_{34} = (1-\kappa)\gamma, l_{44} = d_4, l_{35} = \gamma\kappa, l_{55} = d_2, l_{45} = \psi$, provided (22) holds.

Since the derivative dL/dt is negative definite for any initial point belonging to $\mathbb{R}^5_+$, therefore the endemic equilibrium point is globally asymptotically stable.

4. Sensitivity Analysis for $R_0(\nu)$

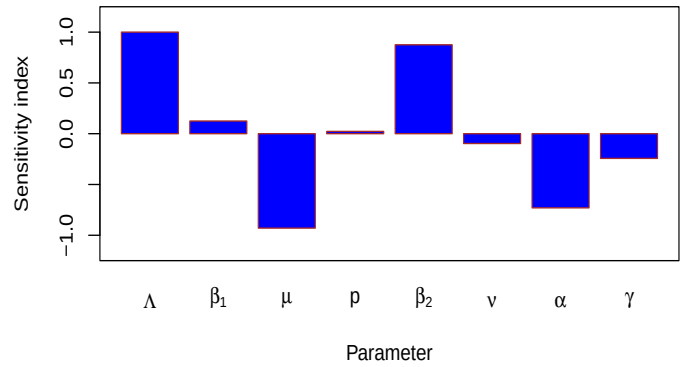

Figure 2: Normalized sensitivity index of $R_0(\nu)$ for parameters involved.

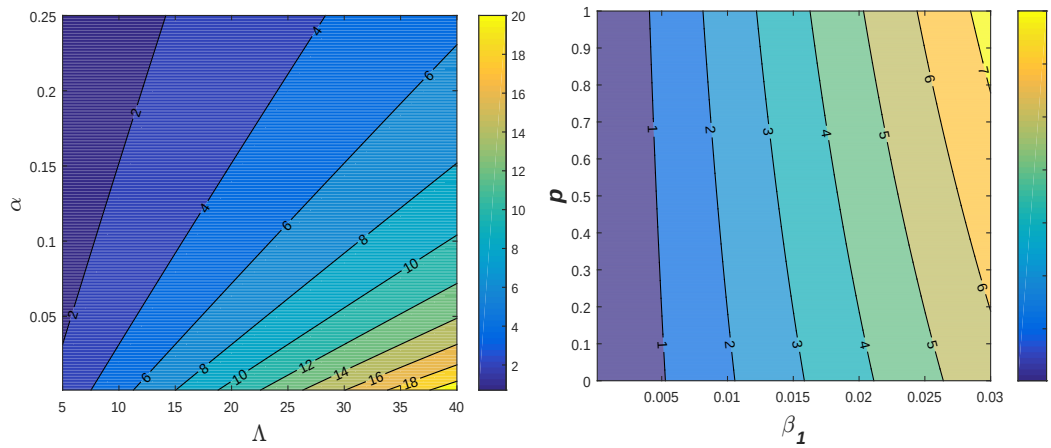

Figure 3: Contour plot of $R_0(\nu)$ as a function of (a) Λ and α (left panel), (b) β_1 and p (right panel).

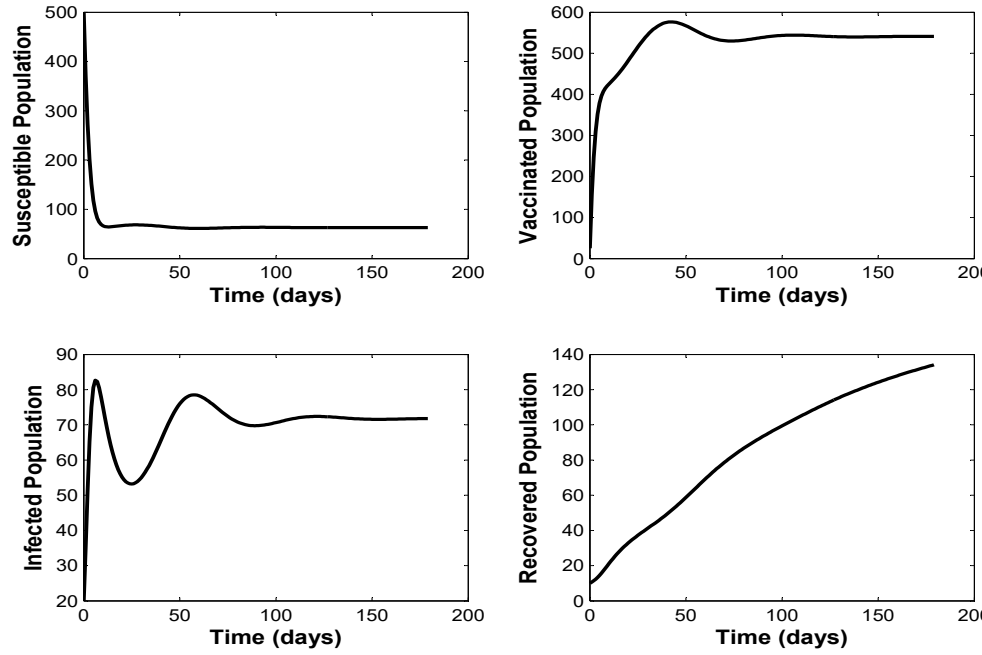

Figure 4: Dynamical behavior of the population showing the trajectory of the system (1) approaches to EE point for the values of the parameters in the Table 1 such that $R_0(\nu) = 4.3 > 1$.

The robustness of the effective reproduction number $R_0(\nu)$ with respect to the fluctuation in the system parameters is explained by carrying out sensitivity analysis. Additionally, it enables us to determine the proportional change in a state variable when a system parameter varies. The following definition is applied to determine normalized forward sensitivity index $\left(S_\theta^{R_0}\right)$ for $R_0(\nu)$ with respect to the parameter θ [17]:

$$S_\theta^{R_0} = \frac{\partial R_0}{\partial \theta} \times \frac{\theta}{R_0}$$

Using the explicit expression for $R_0(\nu)$ in (14), we derive expression for sensitivity indices of $R_0(\nu), S_\theta^{R_0}$ and the corresponding value for each of eight parameters are listed in Table 1.

Table 2: Sensitivity indices of $R_0(\nu)$ taking baseline parameters value from the Table 1.

Parameter	Λ	β_1	μ	p	β_2	ν	α	γ
Sensitivity Indices	1	0.1246	- 0.9295	0.02269	0.8754	-0.0967	-0.7303	-0.2433

Table 2 demonstrates that some of the indices are positive and others are negative, indicating that the indices with " + " sign increase the value of $R_0(\nu)$ as we increase them and those with " − " sign reduce the value of $R_0(\nu)$ as they are increased. The most sensitive positive parameters in decreasing order are recruitment rate (Λ), the disease transmission coefficients (β_1, β_2), probability that an individual has been vaccinated (p). However, Λ has highest positive sensitivity index, its value can not be manipulated effectively practically. $S_{\beta_2}^{R_0} = 0.8754$ indicates that increasing β_2 by 10% will increase $R_0(\nu)$ by 8.8754%. Also, $S_{\nu}^{R_0} = -0.0967$ indicates that increasing ν by 10 % will decrease $R_0(\nu)$ by 0.967%. In the same way, we can interpret the sensitivity indices of other parameters too.

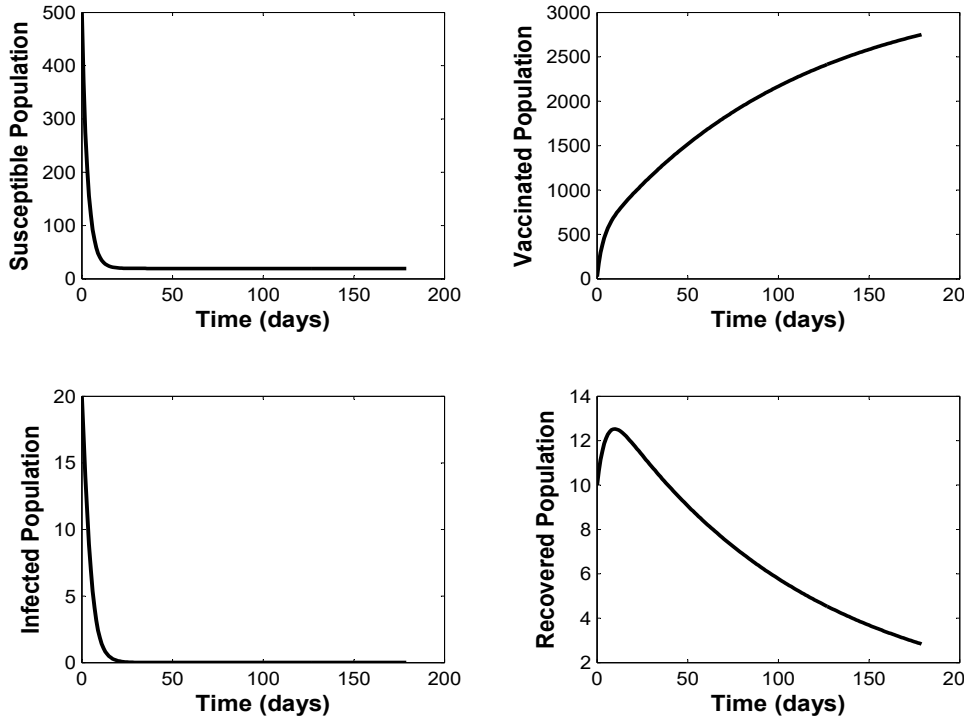

Figure 5: Dynamical behavior of the population for $\beta_1 = 0.001$ and $p = 0.80$ such that $R_0(\nu) = 0.79 < 1$ showing the trajectory of the system (1) approaches to disease-free equilibrium point.

Figure 2 displays sensitivity indices of $R_0(\nu)$ for each of the model parameters using baseline values in Table 2. To control the coronavirus outbreak, we must target the most sensitive parameter. Figure 3 displays contour plots of the effective

reproduction number with respect to the parameters Λ versus α and β_1 versus p. It can be observed from contour that for increasing value of Λ and decreasing value of α, effective reproduction number increases. Again, for increasing values of β_1 and p also increases $R_0(\nu)$. Individuals of susceptible class are continuously shifting to vaccinated compartment with the rate ν and new recruitments enter directly to both susceptible and vaccinated classes. That is why, the parameter β_2 found to be more sensitive than β_1.

5. Numerical Simulation and Discussion

For numerical simulation, we have utilized the reported data about the COVID-19 pandemic in India in current situation. We have adopted some of the values of the parameters from published literatures and others are either estimated or assumed hypothetically. Simulations are carried out taking the initial conditions: $(S(0), V(0), I(0), Q(0), R(0)) = (500, 25, 20, 10, 10)$ and values of the parameters listed in Table 1. The value of the effective reproduction number is calculated as $R_0(\nu) = 4.3$, which is greater than unity and the corresponding trajectories of the model (1) approach to the EE point $E^*(S^*, V^*, I^*, Q^*, R^*)$, explained analytically by the Theorems 3.3, 3.5. Figure 4 demonstrates the scenarios when $R_0(\nu) > 1$; and it is clearly observed that the model possesses an endemic equilibrium in the long run. We can interpret the result as the disease is out of control and cannot extinct.

Using all other parameters values same as in the Table 1 except $\beta_1 = 0.001$ and $p = 0.80$, the effective reproduction number decreases to the value $R_0(\nu) = 0.79 < 1$. The corresponding trajectories of system (1) approaches asymptotically to DFE point as explained in the outcome provided by Theorem 3.4. The nature of the curve representing the populations of different compartments in Figure 5 ensures the obtained outcomes regarding the stability situation at the DFE point in the long run, say 180 days. Figure 6 illustrates the time series of model (1) for the susceptible, vaccinated, infected, quarantined and recovered cases for long run for the different levels of proportion of vaccinated population. It can be observed from Figure 6 that with the increase in fraction of vaccinated population among susceptible class there is significant decrease in number of infected population with oscillation.

In this study, we compare two scenarios: 'Baseline scenario' and 'Force Intervention scenario'. Baseline scenario is the disease dynamical situation with the parameter values as in Table 1, which represent the current status of COVID-19 situation in India. Figure 4 represents baseline scenario of the current scenario unless extra efforts are implemented in the community to decrease transmission rate and to develop immunity capacity of susceptible individuals. The force inter-

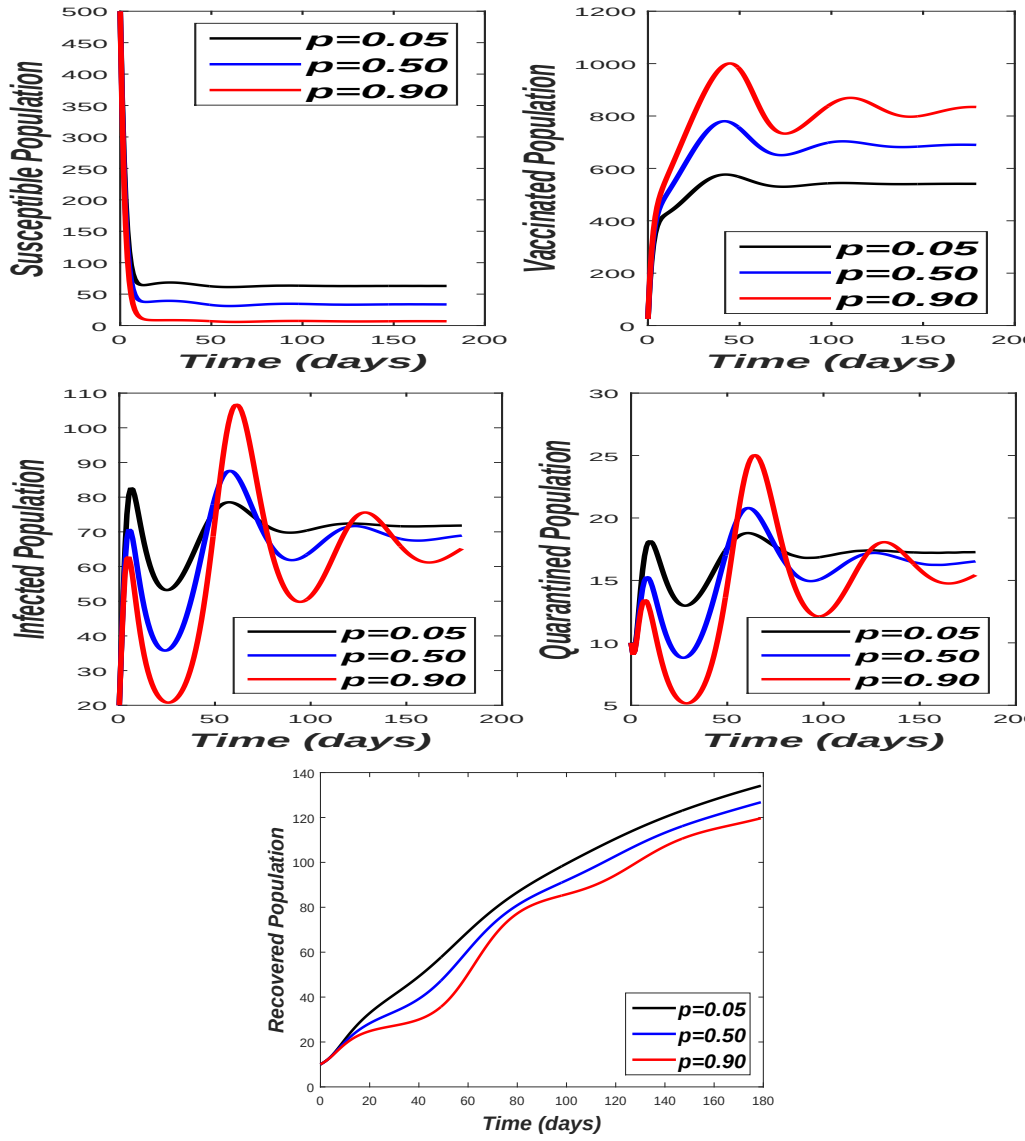

Figure 6: Variation of population for the different levels of proportion of vaccinated population (p).

vention scenario is a hypothetical scenario with extra efforts for control measures and higher percentage of vaccination among population. Figure 6 clears that successive waves can not be avoided without controlling rate of transmission together with mass vaccination campaigns. Assuming 80% population in the community to

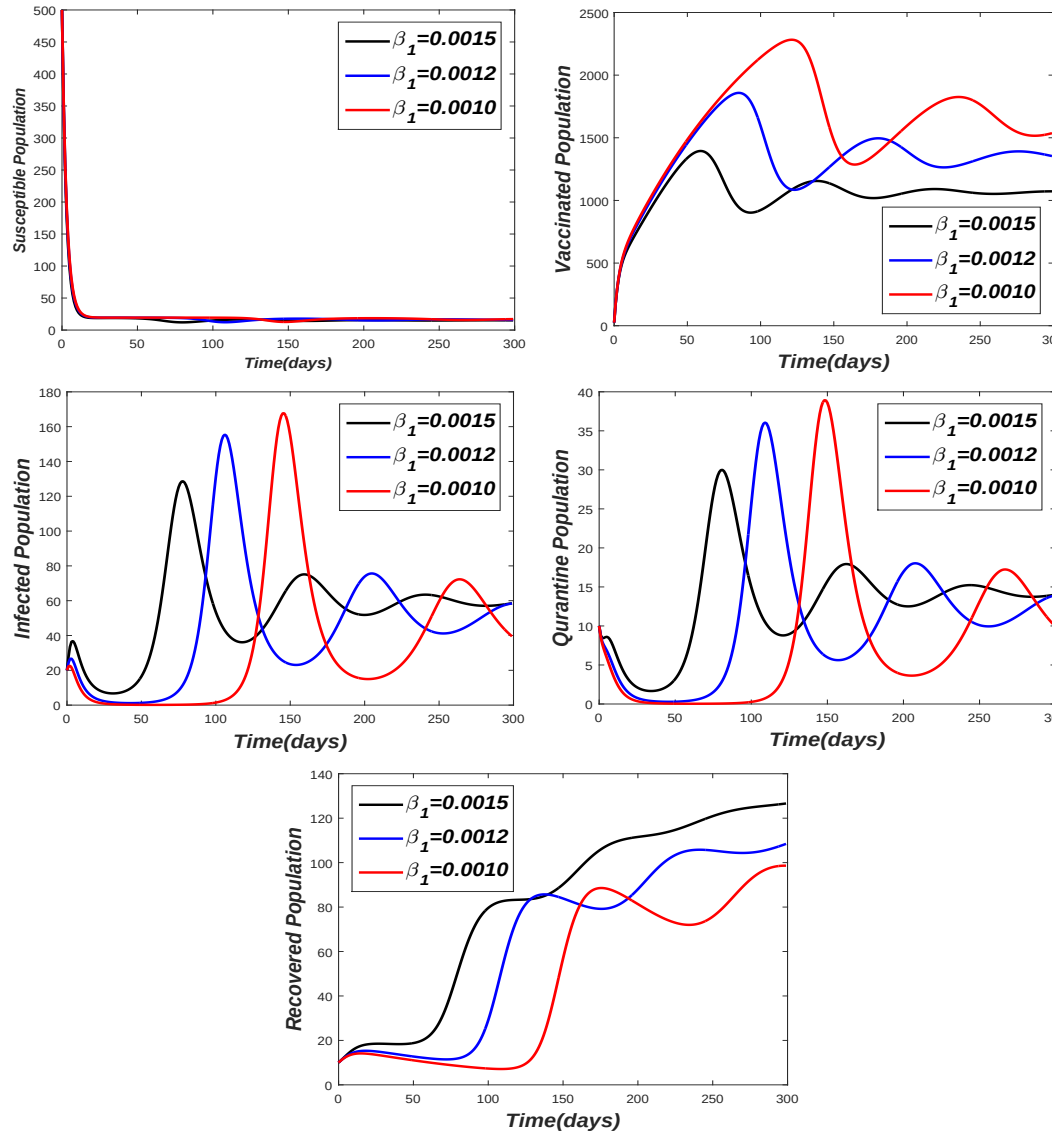

Figure 7: Long term dynamics of human populations in an outbreak, varying the rate of transmission of disease for $p = 0.80$.

be fully vaccinated ($p = 0.80$), we numerically analyze the impact of variation in the disease transmission rate (β_1) by implementing either pharmaceutical or non-pharmaceutical interventions in figure 7. Figure 7 demonstrates that even the huge mass vaccination (80%) to the population could not avoid the successive waves of

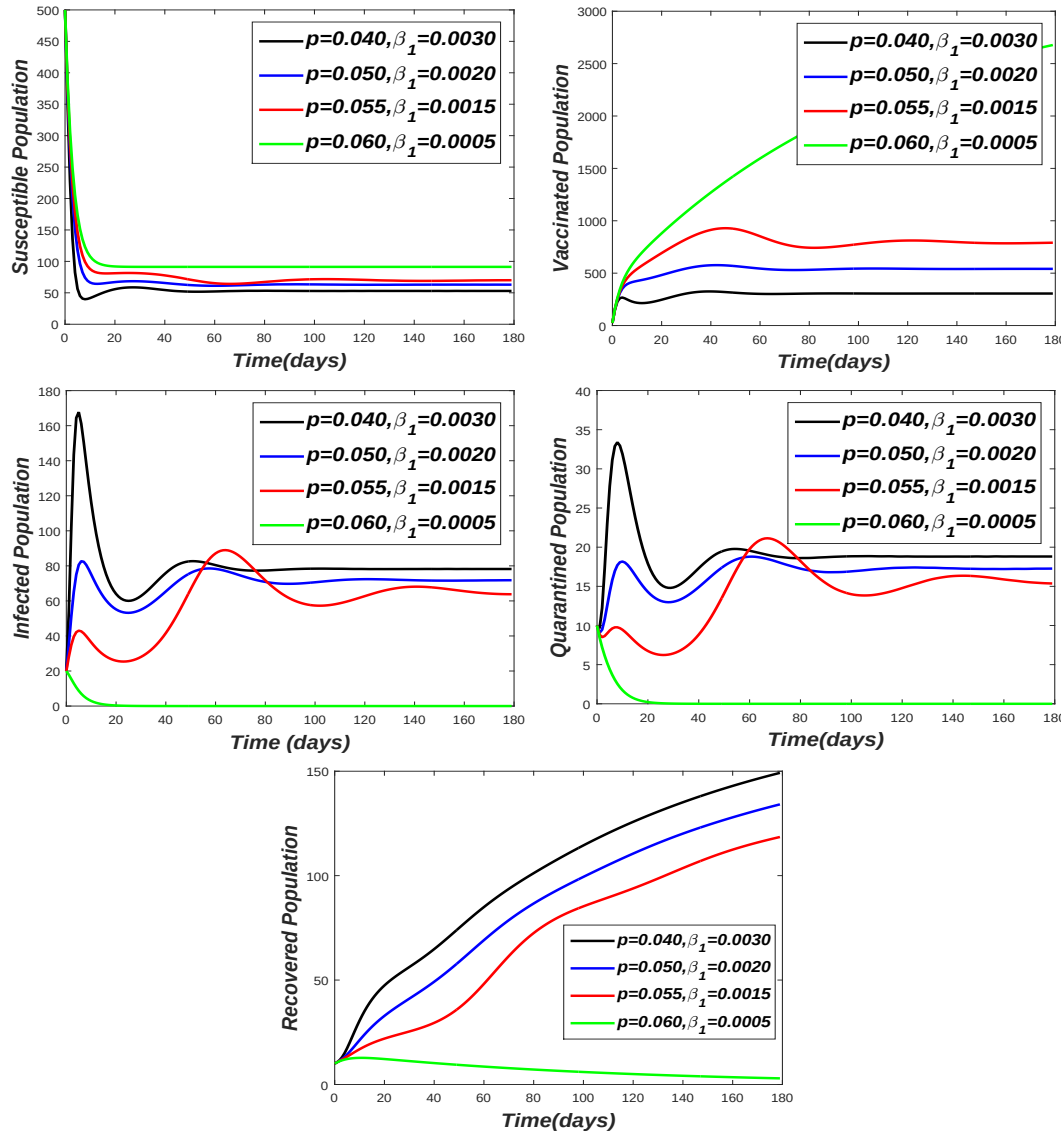

Figure 8: Variation of population for the different levels of proportion of vaccinated population (p) and transmission rate (β_1), other parameters values same as in the Table 1.

the pandemic in future unless we control the rate of disease transmission. For the various values of the parameters β_1 and p, the trajectories of the system (1) are illustrated in Figure 8. It is clear from the Figure 8 that with the increase in the

value of p and decrease in the value of β_1 in some extent, the trajectories still settled at endemic equilibrium point, however quarantined, recovered populations increased too. This indicates that vaccination only could not mitigate or eradicate the disease completely in the current situation. When other interventions are also implemented simultaneously with vaccination to reduce β_1 significantly, the infective population can be controlled.

The simulation results of the model based on the reported data about the COVID-19 pandemic in India, reveal that strict social-distancing, the use of mask and hand sanitizer are necessary to control the rapid spread of disease. The model results also make sure the benefits of mass vaccination as far as authorities can conduct it. We believe those indications can be useful to control the pandemic in India, as well as in other countries where the third wave of coronavirus disease is still in initial stage to spread. The model confirms that diagnosis campaigns can reduce the peak of infection as the diagnosed people undergo quarantine and making them less likely to affect the susceptible population and help to control the epidemic more quickly.

6. Conclusion

We have presented an SVIQR model for COVID-19 outbreak. The impact of vaccination and other controlling measures on the dynamics of coronavirus disease are analyzed. Regarding the expansion of vaccination campaigns around the world, it is one of the significant measures taken to combat the threat posed by the new strain, and the effectiveness of these campaigns is graphically demonstrated. Furthermore, we analyzed the graphical results and found that the increase in coronavirus cases of third strain can effectively be controlled if other control measures are implemented simultaneously. Thus, the pandemic will be under the control by intensifying the mass vaccination campaigns as well as implementing different strategies into practice such as maintaining physical distance, wearing mask, keeping rooms well ventilated, avoiding crowds, washing hands and coughing into a bent elbow or tissue to significantly reduce the number of infected cases. The proposed model can be applied as a planning, preparation and decision making tool by health authorities to control pandemic.

Acknowledgment

The work of Laxman Bahadur Kunwar is partially supported by UGC Nepal under grant "PhD Fellowship and Research Support" (Award No. PhD/76-77 S&T-18).

References

[1] Asamoah, J. K. K., Jim, Z., Seidu, B., Sun, G. Q., Oduro, F. T., Alzahrani,

F., A mathematical model and sensitivity assessment of Covid-19 outbreak for ghana and egypt, Available at SSRN 3612877 (2020).

[2] Babaei, A., Jafari, H., Banihashemi, S., Ahmadi, M., Mathematical analysis of a stochastic model for spread of coronavirus, Chaos, Solitons & Fractals, 144 (2021), 110788.

[3] Bhadauria, A. S., Verma, V. S., Verma, V., Rana, V., An SIQV mathematical model on Covid-19 with virus population in the environment, Mathematics in Engineering Sciences & Aerospace (MESA), 13 (1) (2022), 199-215.

[4] Birkhoff, G., Rota, G. C., Ordinary differential equations, Volume 4, Wiley New York, 1978.

[5] Cai, Y., Kang, Y., Banerjee, M., Wang, W., A stochastic SIRS epidemic model with infectious forces under intervention strategies, Journal of Differential Equations, 259 (2015), 7463-7502.

[6] Chen, G., Li, T., Stability of stochastic delayed SIR model, Stochastic and Dynamics, 9 (2009), 231-252.

[7] Deressa, C. T., Mussa, O., Duressa, G. F., Optimal control and sensitivity analysis for transmission dynamics of coronavirus, Results in Physics, 19 (2020), 103642.

[8] Diekmann, O., Heesterbeek, J., Roberts, M. G., The construction of next generation matrices for compartmental epidemic models, Journal of the Royal Society Interface, 7 (2010), 873-885.

[9] Driessche, P. V. den, Watmough, Reproduction numbers and subthreshold endemic equilibria for compartmental models of disease transmission, Mathematical Biosciences, 180 (2002), 29-48.

[10] Fanelli, D., Piazza, F., Analysis and forecast of Covid-19 spreading in China, Italy and France, Chaos, Solitons & Fractals, 134 (2020), 109761.

[11] Garba, S. M., Lubuma, M. S., Tsanou, B., Modelling the transmission dynamics of the Covid-19 pandemic in South Africa, Mahematical Biosciences, 328 (2020), 108441.

[12] Khajanchi, S., Sarkar, K. Mondal, J., Nisar, K. S., Abdelwahab, S. F., Mathematical modelling of the Covid-19 pandemic with intervention strategies, Results in Physics, 25 (2021), 104285.

[13] Kunwar, L. B., Mathematical modelling of transmission dynamics of Covid-19: A case study of Nepal, Prithivi Academic Journal, (2020), 19-38.

[14] Kunwar, L. B., Verma, V. S., Mathematical modelling of Covid-19 pandemic in Nepal using logistic growth model, Int. J. Grad. Res. Rev., 7 (1) (2021), 17-24.

[15] Liu, J., Wei, F., Dynamics of stochastic SEIS epidemic model with varying population size, Physica A: Stochastical Mechanics and its Applications, 464 (2016), 241-250.

[16] Papachristodoulou, A., Prajna, S., On the construction of lyapunov functions using the sum of squares decomposition, in: Proceeding of the 41st IEEE Conference on Decision and Control, 2002, 3 (2002), 3482-3487.

[17] Rois, M. A., Trisilowati, T., Habibah, U., Local stability analysis of Covid-19 epidemic with quarantine and isolation using normalized index, Telmatika, 14 (2021), 13-24.

[18] Sahoo, B. K., Sapra, B. K., A data driven epidemic model to analyse the lockdown effect and predict the course of Covid-19 progress in India, Chaos, Solitons & Fractals, 139 (2020), 110034.

[19] Sigal, R., Algorithms for the Routh-Hurwitz stability test, Mathematical and Computer Modelling, 13 (1990), 69-77.

[20] Wei, F. Lin, Q., Extinction and distribution for an SIQS epidemic model with quarantined-adjusted incidence, Acta Mathematica Scientia, 37 (2017), 1148-1161.

[21] Yavuz, M., Cosar, F. O., Gunay, F., Ozdemir, F. N., A new mathematical modeling of the Covid-19 pandemic including the vaccination campaign, Open Journal of Modelling and Simulation, 9 (2021), 299-321.

[22] Zhang, T., Teng, Z., Extinction and permanence for a pulse vaccination delayed SEIRS epidemic model, Chaos, Solutions & Fractals, 39 (2009), 2511-2425.

[23] Zhang, T., Peermanence and extinction in a nonautonomous discrete SIRVS epidemic model with vaccination, Applied Mathematics and Computation, 271 (2015), 716-720.